Design and manufacturing of supercritical drying autoclave for aerogel production

Wesam A. A. Twej, Ashraf M. Alattar

Department of Physics, College of Science, University of Baghdad, Baghdad, Iraq

E-mail: asraf_alattar2000@yahoo.com

Abstract

This article will address autoclave design considerations and manufacturing working with high pressure low temperature supercritical drying technique to produce silica aerogel. The design elects carbon dioxide as a supercritical fluid (31.7 ^{o}C and 72.3 bar). Both temperature and pressure have independently controlling facility through present design. The autoclave was light weight (4.5 kg) and factory-made from stainless steel. It contains a high pressure window for monitoring both transfer carbon dioxide gas to liquid carbon dioxide and watching supercritical drying via aerogel preparation process. In this work aerogel samples were prepared and the true apparent densities, total pore volume and pore size distribution, BET surface area, spectroscopic refractive index, structure and thermal properties have been systematically investigated characteristic.

Key words

Autoclave, aerogel, supercritical.

Article info.

Received: May. 2016
Accepted: Sep. 2016
Published: Dec. 2016

تصميم وتصنيع اوتوكليف التجفيف فوق الحرج لإنتاج ايروجيل (الهلام الهوائي)

وسام عبد علي تويج، اشرف محمد ابراهيم

قسم الفيزياء، كلية العلوم، جامعة بغداد، بغداد، العراق

الخلاصة

هذا العمل يقدم تصميم صناعة اوتوكليف ذو ضغط عالي وحرارة منخفضة بتقنية التجفيف فوق الحرج لإنتاج السيليكا ايروجل. تبنى هذا التصميم ثاني اوكسيد الكربون السائل والذي درجة حرارته الحرجة (31.7 م و ضغط 72.3 جو). يكون التحكم، من خلال التصميم الحالي، بدرجة الحرارة والضغط بصورة مستقلة. الاوتوكليف ذو وزن خفيف (4.5 كغم) ومصنعة من مادة الستنليس ستيل. يحتوي الاوتوكليف على نافذة ضغط عالي من اجل مراقبة كل من تحول غاز ثنائي اوكسيد الكربون إلى سائل ثنائي اوكسيد الكربون ومشاهدة التجفيف فوق الحرج أثناء عملية تحضير الايروجل. في هذا العمل تم تحضير نماذج من مادة الايروجل وأجريت قياسات لكل من الكثافة الحقيقية، حجم المسام الكلي وتوزيع حجم المسام، مساحه السطح، الخصائص الطيفية ،معامل الانكسار،خصائص التركيبية والحرارية.

Introduction

Since last decades, autoclaves are used in many variety fields; scientific, medical and industry. Medical device and waste sterilization, architectural glass lamination and automotive, rubber processing and wood treatments are just a few industries that utilize autoclave processing. Our autoclave design will have used to produce silica aerogel material through sol-gel technique by supercritical drying method. Aerogels are considered among the lightest and highly porous solid materials known. Aerogel can be created by combining each of a polymer with solvent to forming the gel, then the liquid inside the pores of gel will be removing and replacing by air. silica aerogels are highly porous and very light materials that are intriguingly and complexly networked

with high specific surface area, low refractive index, low thermal conductivity and low dielectric constant with many fascinating of optical properties all these features make the aerogel ideal choice for different applications. Further, among all aerogels, silica aerogels have become quite popular because they possess a wide variety of exceptional properties such as low thermal conductivity (∼0.01 W/m. K), high porosity (∼99%), high optical transmission (99%) in the visible region, high specific surface area (1000m2/g), low dielectric constant (∼1.0–2.0), low refractive index (∼1.05), and low sound velocity (100 m/s) [1–4]. in the early 1930, Aerogels were first made by Samuel. He dried his waterglass-derived silica gels, employing a solvent exchange and using supercritical conditions to remove the pore fluid (methanol) nondestructively [5]. Three main routs Supercritical drying, ambient pressure drying and freeze drying are methods of producing aerogel. In other hand, the aerogel divided in two type hydrophobic and hydrophilic. In our work producing aerogel hydrophilic by using low temperature supercritical drying with co_2 gas (LTSCD). Supercritical drying is a process to remove liquid in a precise and controlled way. Gel dried at critical point to eliminate the capillary forces that accurse during drying step. When the liquid starts to evaporate from the gel, surface tension creates concave menisci, with continuously of liquid evaporation the compressive forces build up around the perimeter of the pore and contrast. Eventually, surface tension causes the collapse of the gel body [6]. Through heating and compressing the sol-gel above the critical temperature and pressure of the solvent will eliminate the solvent from the sol-gel without generating a two-phase system and also related the capillary forces. Therefore, during conventional thermal drying the gel undergoes cracking and significant shrinkage (up to a few times its initial volume). To eliminate fluids is used supercritical drying without capillary forces [7,8]. Using organic solvents are completely dissolved in ad SC fluid medium. Therefore, prior to SC drying, the solvent is replaced by an alcohol (methanol, ethanol, isopropanol). Thus, during drying, the medium is composed of a single phase therefore, the capillary forces are eliminated [8]. The obtaining an aerogel in sol gel process by removal the solvent from three dimensional network with minimum shrinkage be the most crucial in this work by supercritical drying with CO_2 liquid.

Experimental

1. Materials for autoclave manufacturing

The main parts used in the manufacturing of autoclave were, a tube of stainless steel bear high pressure (Japan), input valves controlling the gas through tube to chamber (china), electronic thermocouple (German), chamber 18 cm in diameter and 35 cm in length (Iraq), 2 pressure gauge reader (Italy), output valve for depressurizing (china).

2. Materials for silica aerogel preparing

The chemicals used in the synthesis were, tetraethylorthosilicate (TEOS) with> 99.0% purity), spectroscopic grade ethyl alcohol (200 proof > 99.5% purity, N, N, dimethaylformamide (C_3H_7NO)> 99.0% purity) deionized water catalyzed by ammonium fluoride (> 98.0% purity) all supplied from Sigma Aldrich. Deionized water catalyzed by hydrochloric acid (0.15 M,> 99.0% purity, Amresco), deionized water catalyzed by

ammonium hydroxide (28-30% concentration, BDH).

3. Procedure

3.1 Design of autoclave

The main part of supercritical drying system is the autoclave, which was one of the major challenges in this work. Special design should be utilizing for providing high pressure sustaining capability that required for achieving supercritical drying. Therefore, before designing and manufacturing the autoclave, well understand of basic autoclave operating principles should be taking into consideration. As example corrosion, stress and fatigue that can weaken the autoclave over time. Therefore, suitable manufacturing metal such as stainless steel had to be picking out. Furthermore, autoclave thickness must be selected carefully, i.e., balancing between good stiffness and well heat transfer.

According to the experimental obstacles and challenges, three autoclave types were designed and implemented in this work.

First design was big size, tightly closed and steely manufactured autoclave; it has the ability to contain large samples and withstand high pressures. One minor inconvenience in this design is that it was without window. Monitoring and watching aerogel preparation under supercritical condition was prevented in this design. The information about temperature and pressure as well as measuring critical point was not recorded precisely, Because of the inability to monitoring the supercritical drying. The good and saved robust advantage was associated with some disadvantages such as; the size of autoclave make the thermal controlling through the preparation process so difficult and the process was associated with high consumption of CO_2 gas amount and time.

The shortcoming in the first autoclave designed was lead about new autoclave. The previous stumbles were overcome by means of adding quartz window and by decreasing the device size as well as stainless steel material was employed. These improvements give way to a good monitoring and controlling abilities. Through this autoclave type, the first process of supercritical drying has been watching and recording, moreover our first suitable aerogel sample was achieved.

However, the difficulties were started again. Where, because of the exterior hater and thermocouple, in the second type design, the accurate control of heat convert from the ambient to critical temperatures was poor. Hence, this type of autoclave was made of stainless steel; therefore, it was highly influenced by the heat surrounding. In addition to the lack in controlling, the pressure rises and downing, as well as keeping the samples inside for a long time, during supercritical drying process.

Although, several succeeded aerogel samples were utilized from the second autoclave, still few modifications were required. These modifications make the process easier and precise in order to obtain aerogel samples of uniform geometrical shape and also to make best controlling on the final product properties.

The third autoclave system designed was including, inside the heart of the autoclave, thermocouple type thermometer and pyrometer for recording the temperature and pressure respectively as shown in Fig. 1.

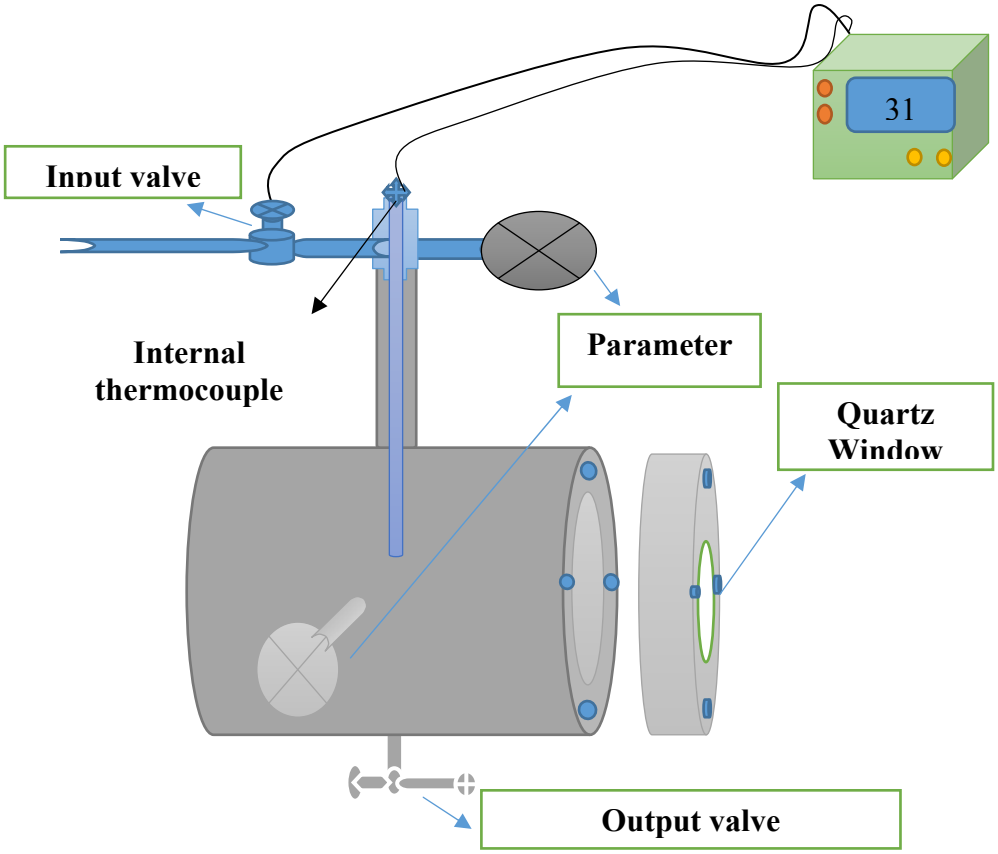

Fig.1: Simple scheme of the third type autoclave.

The last implemented autoclave, third designed, was unable us making the process performance more softly. Pressurization, Autoclaves be pressurized with CO_2 gas and make test on it till 2185 psi to be sure that will work good at higher pressures. Proportional vessel pressurization control valves were also tested well before used. Two safety valves are implemented in this autoclave, on top for input and an air vent on the bottom with slow depressurizing and smooth in controlling. Thermocouple channels go inside the autoclave and deep till middle of the diameter that gave the real temperature inside the autoclave during heating and cooling. Two Pressure-gauges were adding too, this will help us to give the real pressure in the autoclave and reach to supercritical point and that is our goal. Thus during the supercritical drying it is compulsory to provide optimum mixing between CO_2 and supercritical drying and the solvent in the pores of the gel, through all of these steps we optimize the drying time. It should be in the gel during the process necessary to hinder the formation of zones with significantly different solvent concentrations. In addition, it had been making a window for viewing and control of the operation to be obtained. To achieve this result, the distribution of the flow rates of supercritical CO_2 within the gel must be as uniform as possible. Fig. 2 illustrates the third autoclave type photo.

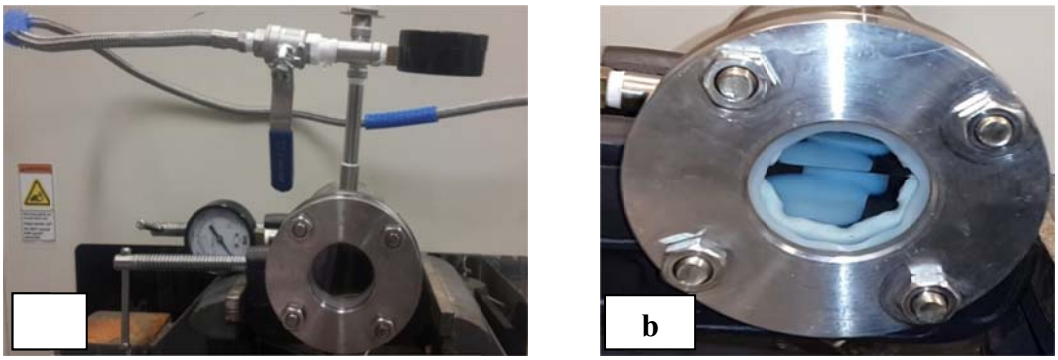

Fig. 2: Camera photo of the third type autoclave (a) all system, (b) samples under supercritical condition inside the autoclave.

3.2 Silica aerogel preparation procedure

Silica gels were prepared via a single-step procedure as following; tetraethylorthosilicate (TEOS), ethanol, water, and hydrochloric acid or NH_4OH (molar ratios 1:12:11: C) where C was varied to achieve final sol of pH under magnetic stirring. The sols were heated at 303 ^{0}K for 30min. Next, 0.5 ml of C_3H_7NO, was adding as drying control chemical additive (DCCA), then left for further one hour under magnetic stirring. The resulting sol was allowed to gel in 2.45 cm diameter plastic tubes and then aged in the same tubes for 28 h at room temperature. In order to remove any unreacted monomer from the gel network, the gels were washed with pure ethanol in five 24 h steps, using fresh ethanol for each successive step. Silica aerogel prepared from the same silica gel in the first stage by using supercritical drying technique (low temperature carbon dioxide solvent exchange). Where the alcogel is placed inside the autoclave while at the same time that the sample be moist and under constant drenching with ethanol for 30 minutes and closed the autoclave very well. The CO_2 gas pumping into the autoclave very slowly until reaching the pressure of 55 bar with the synchronization process cooling autoclaving also at the same time for transfer the CO_2 phase from gas to liquid. Over this process, it will be noted that the liquid was separated into two manifest parts. Keeping these two liquids stable for proper time then changing the liquid CO_2 more than 4 times for 28h to vent all the water and other solvents out the gel making the alcogel soaking in liquid CO_2 only for more 36 h. Start heating process by increasing the autoclave temperature, using wire heater, slowly to obtain supercritical condition at 73 bar and 32 ^{0}C. Maintain the temperature in the information boundary operation of supercritical drying for 2 hours to 3 hours with depressurizing for this process every 30 minute while keeping the temperature and pressure above supercritical boundary. Finally, depressurizing process have allowed continuing for few hours to get the uniform shape silica aerogel.

All these samples are kept in an oven for an hour within 700 ^{0}C. After densification found there is difference in density of sample.

4. Characterization method of aerogels

Pore size distribution and specific surface area of aerogel sample were determined by the BET method (Micromeritics ASAP 2020). Fourier transform infrared (FTIR) type is Nicolet Is50 used to confirm the surface silylation of the aerogel. UV-VIS spectrophotometer (Ultrospec. 4300 pro) was used in this work to

record the transmittance of the aerogel sample.
The morphology and microstructure of silica aerogel samples were observed by scanning electron microscopy (SEM, ULTRA 60) in secondary electron mode. The dried aerogel then heated to 700 °C at a rate of 60 °C h^{-1}.

Results

1. Surface area and pore size measurement.

BET nitrogen adsorption-desorption was used to obtain pore volumes and surface areas of the silica aerogel. A BET analysis from the amount of N_2 gas adsorbed at various partial pressures (five points 0.05 <P/Po < 0.35, a single condensation point (P/Po = 0.99) was used to find the pore size and pore volume.
Fig. 3 presents the linear isotherm plot for the aerogel sample pH1.

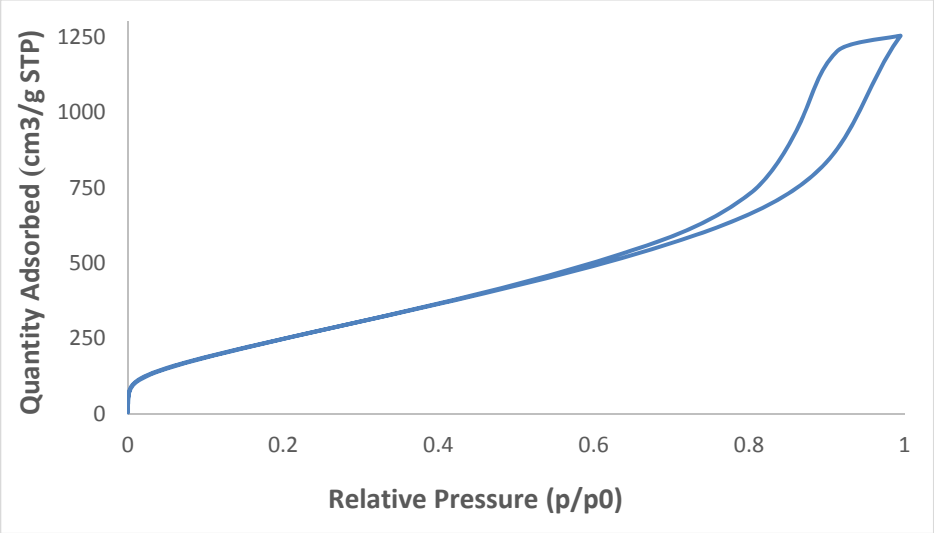

Fig. 3: Linear isotherm plot for aerogel prepared at initial pH1.

Table 1: The results surface area, pore volume and pore size of silica aerogel produce by supercritical drying.

Table 1: The nitrogen sorption measurement for silica aerogel											
pH	Surface area (m^2 / gm)				Pore volume (cm^3 / gm)			Pore size (A°)			Porosity %
	single	BET	BJH Ads	BJH Des	single	BJH Ads	BJH Des	BET	BJH Ads	BJH Des	
1	934	998	1011	1105	1.93	1.79	1.82	77.71	71.01	65.93	86.33

From Table 1 and Fig. 3 show the high specific surface area 998 with high porosity of the silica aerogel pH1. The porosity result was calculated after calculating the density of sample from their mass to volume ratio, the porosity percentage of sample was estimated to the following equation:

$$\text{Porosity } (\%) = \left(1 - \frac{\rho b}{\rho s}\right) \times 100, \qquad (1)$$

where ρb is the bulk density of synthesized silica aerogel and ρs is the density of silica skeleton.
Table 2 presents the measured mass, dimensions and densities of gel and aerogel samples. This table illustrates aerogel density before and after densification at 700 ^{0}C.

Table 2: Dimensions, mass and densities of prepared samples.					
sample	Mass (gm)	Radius (cm)	High (cm)	Volume (cm^3)	Density $\mathcal{D}_\rho$ (g/cm^3)
gel	6.392	2.9	0.95	6.277	1.02
Aerogel before dandification	0.238	2.7	0.75	4.296	0.055
Aerogel after dandified at 700 ^0C	0.217	2.7	0.75	4.296	0.05

2. FT-IR

Fig. 4 shows the FTIR spectra of the silica aerogel synthesized at pH1 with 700 ^0C for densification temperature.

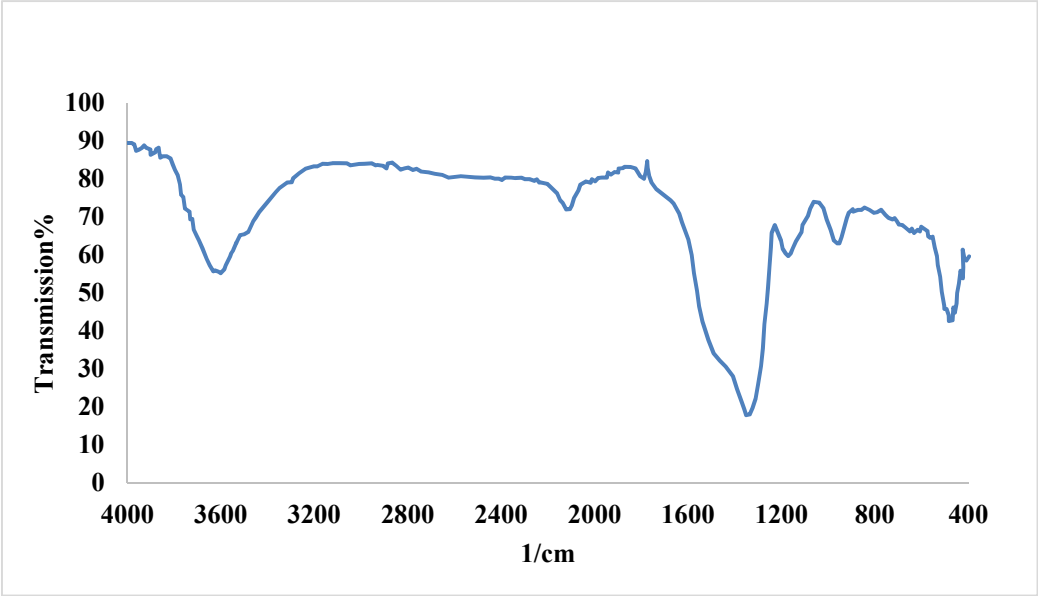

Fig. 4: FTIR spectrum of the prepared aerogel.

3. UV-VIS

The Fig. 5 show the transmittance of silica aerogel sample produce by supercritical drying as function of wavelength at final pH1 value. In addition, the optical image (Fig. 6) shows the transmittance of the specimen produced by supercritical method.

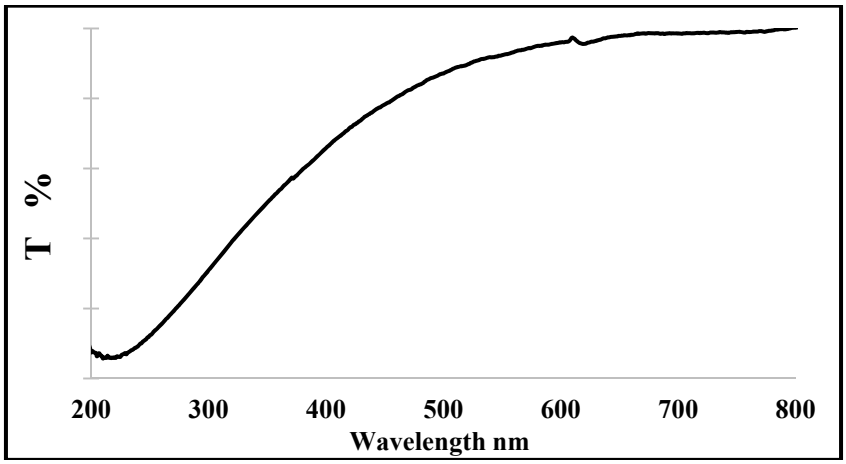

Fig. 5: Transmittance spectra of aerogel sample at pH1.

Fig. 6: Camera photo for (a) aerogel sample pH1 on black background (b) various pH value samples on white background.

4. Morphology

Fig. 7 Show SEM images for silica aerogel sample, it can be seen distribution of the porous shows narrow pore size distribution. The pore size of pH1 is equal from (6.6-9 nm). This result it's confirmed with the result of BET Table 1 and pore size distribution. This figure show also the core of aerogel is open cellular foam. In other hand, the morphology image shows the pH1 have ultrafine structure at surface and the side show that structure its defined as foam.

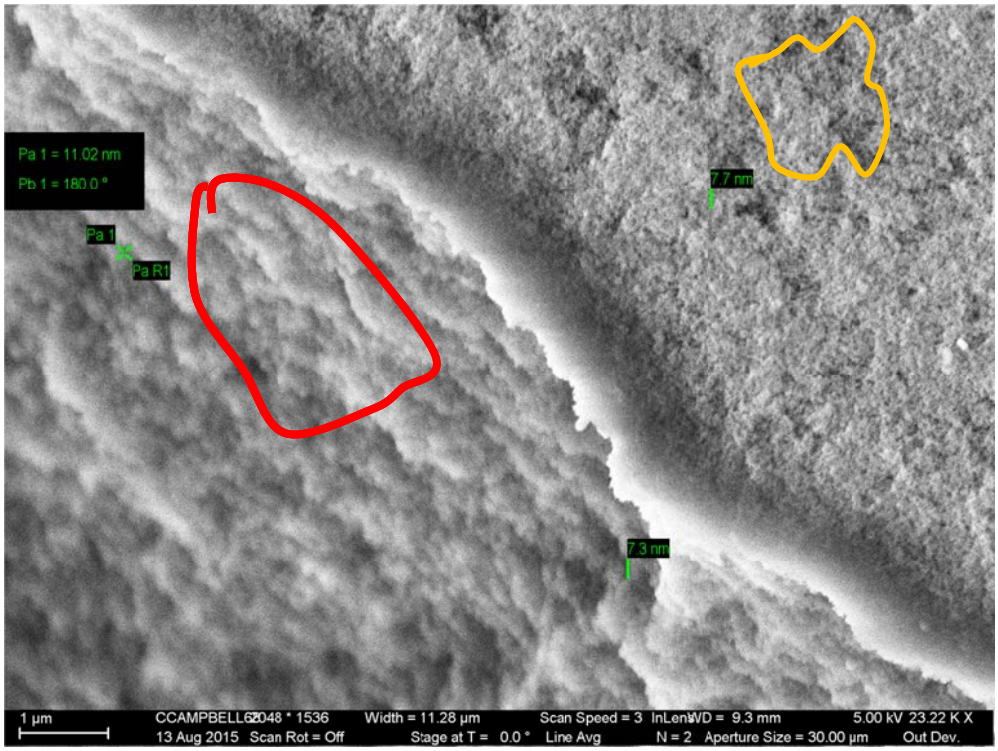

Fig. 7: SEM image for aerogel sample.

5. Refractive index

Fig. 8 show the refractive index of the silica by using Ellipsometer device the refractive index measured for silica network was n = 1.4585. In other hand, the Ellipsometer give the refractive index for specimen of aerogel silica n= 1.0514 as total refractive index of aerogel sample.

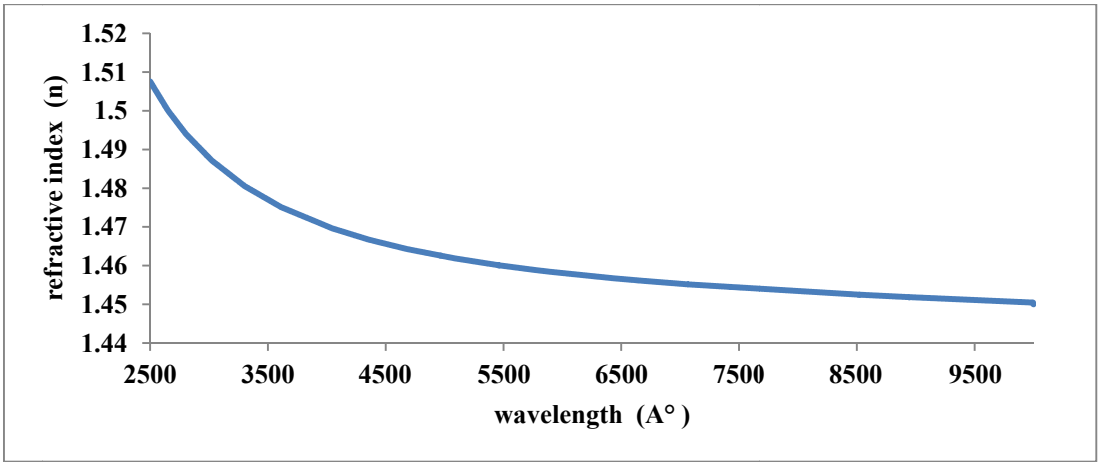

Fig. 8: Refractive index of silica skeleton SiO_2.

6. Energy dispersive spectroscopy

At very high magnifications, especially under high beam currents, aerogel core displays the compositional contrast in the sample and the Fig. 9 shows the distribution of elements in layered material of aerogel bulk. In other hand, spectrum map in the Fig. 10 illustrate the ratio of the elements that existed.

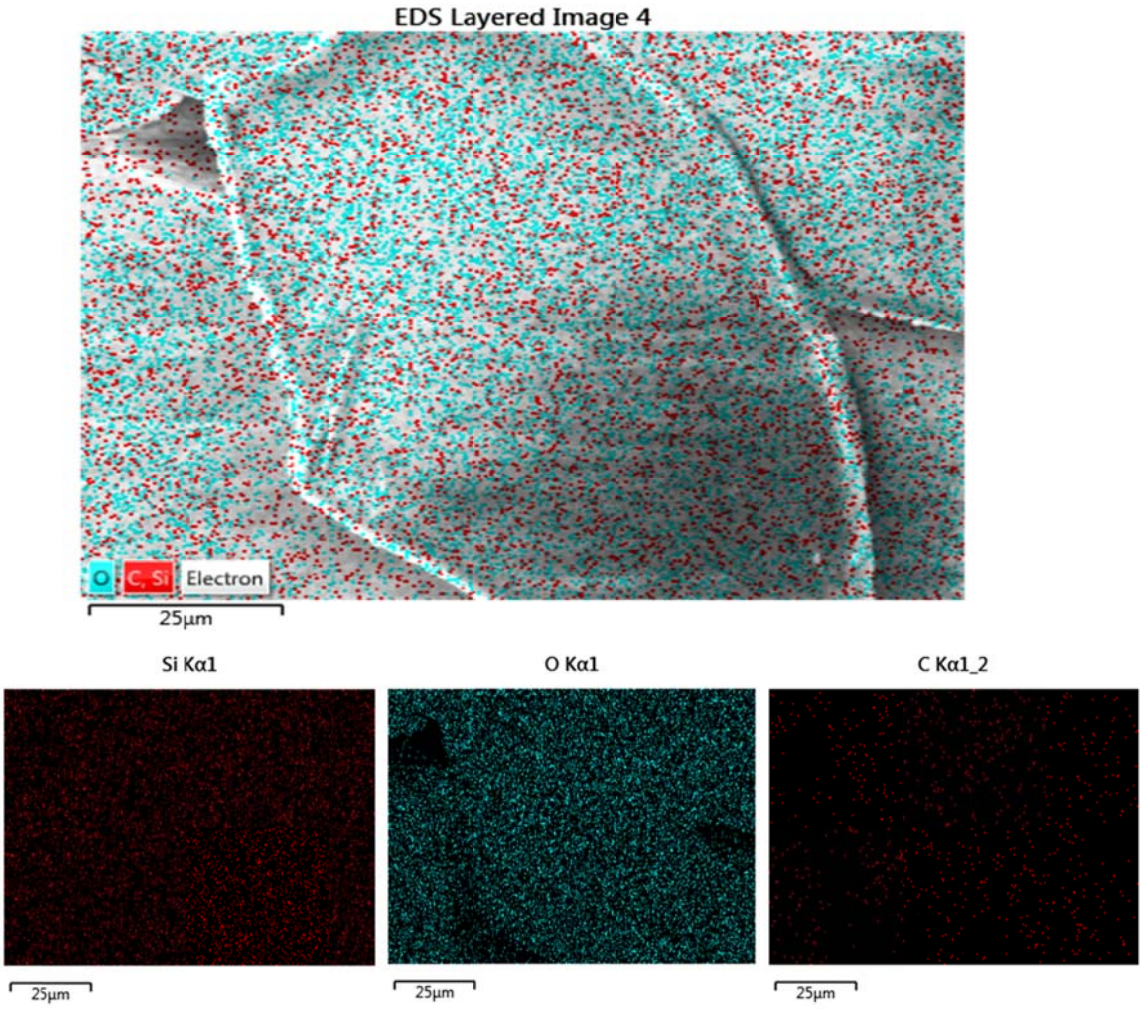

Fig. 9: EDS image for the sample of aerogel PH1.

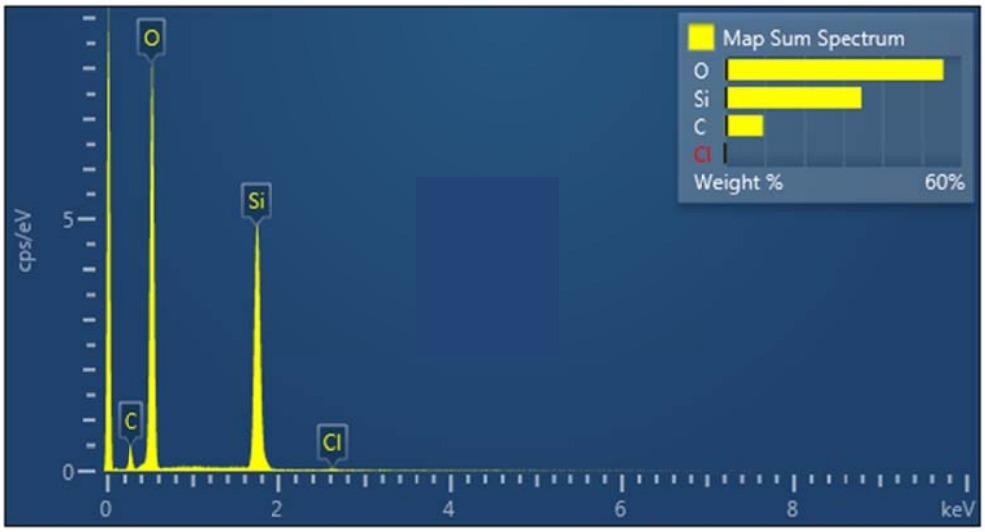

Fig. 10: EDS map sum spectrum for the sample of aerogel PH1.

7. Thermal conductivity via the Lee's Disc

Conductivity experiments were carried out via the Lee's Disc method of aerogel samples. The heat transfers between an aerogel bulk and its surroundings depends on the exposed surface area of the aerogel sample and the temperature difference between the bulk aerogel and its surroundings. Thermal conductivity of aerogel bulk pH1(0.0063 mW m^{-1} ^{0} C^{-1}). The thermal conductivity of the specimen aerogel (λ), thickness h and cross-sectional area of a is given by: [9]

$$\lambda = \frac{h}{a}\frac{\Delta Hf\ (lit)}{\Delta Hf(meas)} Sonset \qquad (2)$$

where ΔHf (lit) is the literature value for the heat of fusion of the metal, ΔHf (meas) the measured value for the heat of fusion of the metal and Sonset is the slope of ΔH/dt versus T for the onset of melting of the standard. The temperature of the aerogel specimen (TS) is the mean temperature of disks A and B. H is the heat supplied from the apparatus by the electrical heater is given by [9].

H= VI (3)

where V is the potential difference across the heater and **I** is the current which flows through it. the heat flowing through the aerogel specimen S is [9] :

$$h_s = \lambda \pi r^2 \frac{TB-TA}{d} \qquad (4)$$

where r is its radius, d its thickness and λ the thermal conductivity of the specimen. when turn on the heater electric, the heat will flow from the heater in to C1 and then from C1 across to the sample aerogel to C3. By emission and convection, the heat will be lost to the environment from the surface area of C1 and C3 and from the rim of C2, the rim of the heater and the rim of aerogel sample. Where C1 is the heater disc, C2 is the sample disc and C3 is the disc receives heat to measure the conductivity.

Discussion

The sol gel parameters were optimized in order to produce aerogel without cracks utilizing supercritical drying technique via eliminating capillary force inside the aerogel pores. In fact, the pressure gradient depends on the characteristics of the fluid flow through the aerogel pores [10] as well

as it also depends on the aerogel structure. During the initial stages of the supercritical CO_2 drying process the diffusion kinetics is the another important factor of the liquid CO_2 – solvent exchange in the autoclave. unsteady-state diffusion of solvent and liquid CO_2 will cause the structural damage at this point, which occurs when liquid CO_2 and the solvent mixture is below the binary critical curve where both liquids are not miscible and exist as two separate phases. Eventually, the supercritical drying will not be able to eliminate the capillary forces in the pores and the fragile aerogel structure will collapse. Under the right conditions in the CO_2 – solvent exchange, liquid CO_2 it will surrounding the specimen of alcogel in the autoclave and the solvent that fills its pores are miscible. The diffusion will take place when two miscible liquids are brought into contact. Fick's first law of diffusion can be rewritten as $J \propto -P(C_2\text{-}C_1)$, where *J* is the rate at which solvent diffuses out through a unit area of the alcogel, *P* is the alcogel permeability, and is the difference in concentration of the solvent across the aerogel in the direction of flow [11]. In other side, it appears that some of the most critical factor the control of structural integrity of aerogel is related to the rates in the supercritical drying process, rate of CO_2-solvent changing and vessel depressurization rate during the process of drying. The specimen in the Fig. 6 appeared extremely perfect, which once again emphasizes the importance of controlling the rate of CO_2 – solvent exchange. Increased cracking in silica aerogels as a result of the quick diffusion of ethanol from gels into the liquid CO_2 was also observed in other studies [12, 13]. The liner isotherm plot which are presented in Fig. 3 can be examine with the aid of the IUPAC classification hysteresis loops [14]. The sample of pH1 aerogel may be classified as H3type which is related to non-rigid aggregates of plate-like particles (slit-shaped pores) shown in Fig. 3. Table 1 show that the silica aerogel produced by supercritical drying have high specific surface area with low pore size, in addition the porosity is high also. The density of silica aerogel measured through the thickness and diameter of the specimen of aerogel bulk show have lowest density 0.0504 this result after finished the densification at 700 ^{0}C, supercritical drying not able to eliminate all the solvent inside the pores.

The Table 2 shows the mass, radius, thickness and density for aerogel bulk sample before and after densification. Through the step of densification, it is observed that there are varied differences in the density of these sample pH value. Also the shrinkage in the radius and thickness after supercritical drying method show volume have big different after drying, in other hand, the difference in the density after densification that all the solvents inside the pores are evaporated under high thermal temperature. From the FTIR graph in Fig. 4 it is clear that the intensity of the bonds at 3452 and 1641 cm^{-1} of O–H groups is less and peak intensities at 941 cm^{-1} related to Si-OH group. Symmetric and asymmetric Si–O–Si stretching vibrations have made the intensified peak at 1085 cm^{-1} and its shoulder at 812 cm^{-1}.

The transmittance of aerogel showing in the Fig. 5 that is best transparency start with visible region to IR. Fig. 7 images of the sample aerogel the morphology of the sample is monostructural, characterized by open cellular foam, this give clearer idea about the structure of the aerogel has different pores size. The surface structure show that the aerogel near to be as fractal and that clear from the

orange circle with different pores distribution and size, while the internal structure show that is already be as open cellular foam that make the transmittance high enough. Fig. 9 show the distributions of the element (SI, C, O and Cl) in the aerogel sample. The process of densification at high temperature has made the catalyst acid that is used in this pH value evaporated and leads to know the catalyst liquid inside the pores are evaporate after densification at high temperature (700^0C). Fig. 10 show that, through EDS image, the Choler ion does not exist in the map. The starting pH, therefore, strongly influences the resulting microstructure and, therefore, allows for the control of microstructure-dictated properties. The influence of temperature densification on the bulk aerogel show the evaporation of liquid through the pores will help more to get lowest density of the material, in other hand that approve the only elements exist inside the bulk it's the silica and carbon oxide. The density of the aerogel materials a play important role in thermal conductivity resulting increases in solid components will decreases the thermal conductivity, thus the lowest density lowest thermal conductivity.

A series of investigations were next undertaken to determine the effect of other variables on the conductivity of silica aerogel, density of the aerogel and 'particle size of the aerogel [15]. For dens silica the solid conductivity is relatively high (a single-pane window transmits a large amount of thermal energy). .in general, the silica aerogel possesses very small (1-10%) fraction of solid silica. the aerogel silica has three dimensional network that make the solids that are present consist of very small particles linked in the aerogel network in three dimensional with many "dead ends". therefore, the thermal transparent through the solid portion of silica aerogel occur through tortuous path and is not particularly effective that will have caused the lowest thermal conductivity of these type of materials. In addition, the porous are not closed of the sample but open that will cause to the gas passage through and that is another reason for lowest conductivity.

Conclusions

In this work, we present simple designed homemade autoclave that can provide aerogel samples of proper physical properties. Autoclave of built-in glass window provides important facility that reveals good thoroughness in determining the actual temperature and pressure at exactly phase separation, i.e. supercritical point. The wise controlling of CO_2 gas flow as well as temperature gradient through supercritical condition reaching process have great influence on the aerogel final shape homogeneity. The microstructure and optical properties of the prepared aerogel can be systematically controlled by means of suitable selection of initial parameters. Density measurement and FTIR mentioned that densification process is play significant roles in identifying the final aerogel structural properties. Therefore, several applications; optical instruments, low densities thermal insulator, small-pore hydrogen storage tanks etc., could be functionally through adjusting starting catalyst.

References

[1] L. W. Hrubesh, Chemistry and Industry, 24 (1990) 824–827.

[2] G. C. Bond and S. Flamerz, Applied Catalysis, 33, 1 (1987) 219–230.

[3] J. Fricke and A. Emmerling, in Structure and Bonding 77: Chemistry, Spectroscopy and Applications of Sol-Gel Glasses, pp., Springer, Berlin, Germany, (1992) 37–87.

[4] C. A. M. Mulder and J. G. Van Lierop, in Aerogels, J. Fricke, Ed., Springer, Berlin, Germany, (1986) 68–75.
[5] S.S. Kistler, "Coherent Expanded Aerogels and Jellies", Nature 127, 741 (1931).
[6] D. M. Smith, G. W. Scherer, J. M. Anderson, Journal of Non-Crystalline Solids, 188, 3 (1995) 191–206.
[7] I. Smirnova, PhD. Thesis (Technical University of Berlin, 2002).
[8] P. A. Gurikov, "Candidate's Dissertations in Technical Sciences" (Russ. Chem. Technol. Univ., Moscow, (2010).
[9] Duncan M. Price, Mark Jarratt, Thermochimica Acta 392–393, 231–236 (2002).
[10] G.W. Scherer: Theory of drying. Journal of the American Ceramic Society 73, (1990) 3-14.
[11] Kalyan Athmuri and Val R. Marinov, insights from a process study, North Dakota State University, Industrial and Manufacturing Engineering, Fargo, ND 58102, USA, Advance in Materials Science, 12, 1 (31), 2012.
[12] G. Rogacki, P. Wawrzyniak, Journal of Non-Crystalline Solids 186, (1995) 73-77.
[13] Z. Novak, Ž. Knez, Journal of Non-Crystalline Solids 221, (1997) 163-169.
[14] K. S. W. Sing, D. H. Everett, R. A. W. Haul, L. Moscou, R. A. Pierotti, J. Rouquerol, T. Siemieniewska, Physical and Biophysical Chemistry 57, 4 (1985) 603–619.
[15] J. F. White, "Silica aerogel Effect of Variables on Its Thermal Conductivity", Industrial and Engineering Chemistry, 31 (1939) 7.